# Kinetic Studies of Adenosine Kinase from L1210 Cells: A Model Enzyme with a Two-Site Ping-Pong Mechanism†

Chi-Hsiung Chang,* Sungman Cha, R. Wallace Brockman, and L. Lee Bennett, Jr.

ABSTRACT: Purified adenosine kinase from L1210 cells displayed substrate inhibition by high concentrations of adenosine (Ado), ATP, and $MgCl_2$. When incubated with ATP and $MgCl_2$, the enzyme was phosphorylated, and the phosphorylated kinase transferred phosphate to adenosine in the absence of ATP and $MgCl_2$. Substrate binding, isotope exchange, and kinetic studies suggested that the enzyme catalyzes the reaction by means of a two-site ping-pong mechanism with the phosphorylated enzyme as an obligatory intermediate. Among many possible pathways within this mechanism probably a random-bi ordered-bi route is the preferred sequence in which the two substrates, adenosine and MgATP, bind in a random order to form the ternary complex MgATP·E·Ado followed by the sequential dissociation of MgADP and AMP. Dissociation constants of various enzyme–substrate and enzyme–product complexes and the first-order rate constant of the rate-limiting step were estimated.

Adenosine kinase (ATP:adenosine 5′-phosphotransferase, EC 2.7.1.20) has been partially purified from a variety of mammalian sources (Caputto, 1951; Lindberg et al., 1967; Schnebli et al., 1967; Murray, 1968; Lindberg, 1969; Divekar & Hakala, 1971; Henderson et al., 1972; Shimizu et al., 1972; Namm & Leader, 1973; Schmidt et al., 1974; DeJong, 1977) and purified to apparent homogeneity from brewer's yeast (Leibach et al., 1971), rabbit liver (Miller et al., 1979), rat brain (Yamada et al., 1980), murine leukemia L1210 cells (Chang et al., 1980), and human liver (Yamada et al., 1981); 3600-fold purification of the kinase of human placenta was also reported (Andres & Fox, 1979). Adenosine kinase and adenosine deaminase are key enzymes in the metabolism of adenosine and its analogues. The absence of adenosine deaminase in immunodeficiency diseases (Fox & Kelley, 1978) and the discovery of potent inhibitors of adenosine deaminase (Schaeffer & Schwender, 1974; Woo et al., 1974) have resulted in intense interest in the metabolism of adenosine, deoxyadenosine, and adenosine analogues and in the kinases responsible for their phosphorylation (Henderson et al., 1980).

The kinetic behavior of the enzyme from Ehrlich ascites tumor cells was studied by Henderson et al. (1972) by using 6-(methylmercapto)purine ribonucleoside as substrate. It was proposed that the enzyme catalyzed an ordered bi-bi reaction with ATP as the first substrate to bind and ADP as the first product to dissociate from the enzyme. Palella et al. (1980) studied the kinetic properties of highly purified human placental adenosine kinase and concluded that the reaction proceeds by an ordered bi-bi addition of substrate and release of products in which adenosine is the first substrate to bind and AMP is the last product released.

Some properties of adenosine kinase purified from L1210 cells have been reported (Chang et al., 1980). In a further study of this kinase we have found that the enzyme is phosphorylated and that the phosphorylated kinase can transfer phosphate to adenosine in the absence of $MgCl_2$ and ATP; this is the first reported evidence for phosphorylated enzyme as an intermediate in the adenosine kinase reaction. This finding indicated the desirability of a full study of the kinetics of this reaction. We report here our evidence for the phosphorylation of the kinase from L1210 cells and the results of kinetic studies that indicate that the enzyme catalyzes a two-site ping-pong reaction pathway with the phosphorylated enzyme as an obligatory intermediate.

## Experimental Procedures

*Materials.* Nucleotides and nucleosides were purchased from Sigma Chemical Co., St. Louis, MO. [8-$^{14}$C]Adenosine was supplied by Moravek Biochemicals, City of Industry, CA. [8-$^{14}$C]ATP and [$\gamma$-$^{32}$P]ATP were obtained from New England Nuclear, Boston, MA. [$^{32}$P]AMP was purchased from Amersham Int. Ltd., Amersham, U.K. All other chemicals were of reagent grade. dGTP–Sepharose was generously provided by Drs. P. J. Hoffmann and R. L. Blakley (1975). Blue–Sepharose, DEAE-cellulose, and octyl-Sepharose was purchased from Pharmacia Fine Chemicals, Piscataway, NJ.

*Enzyme Assay.* Total volume of the enzyme assay mixtures was 0.1 mL and included 50 mM tris(hydroxymethyl)-aminomethane hydrochloride (Tris-HCl), pH 8.0 (4 °C), 6 $\mu$g of bovine serum albumin (BSA), and $MgCl_2$ in 0.4 mM excess of the sum of nucleoside di- and triphosphates. ATP and adenosine concentrations were varied as indicated in the text. The assay mixture was incubated at 37 °C for 1 h; the enzyme reaction was found to be linear with respect to time and enzyme concentration during this incubation period. The reaction was stopped by immersion of incubation tubes in a boiling water bath for 2 min; 50 $\mu$L of the reaction mixture was then spotted on a Whatman DE-81 paper disk. The DE-81 disks were washed 3 times with 2 mM ammonium formate, once with $H_2O$, and once with alcohol. Disks were dried and transferred to scintillation vials; quantitative determinations of radioactivity were made by addition of Scinti-Verse (Fisher Scientific Co., St. Louis, MO) and counting in a Packard Tri-Carb liquid scintillation spectrometer.

*Preparation of the Purified Enzyme.* The source of L1210 ascites tumor cells and the method of purification of adenosine kinase have been described (Chang et al., 1980). The enzyme isolated from the final step of purification (octyl-Sepharose column chromatography) was found to possess NDP kinase

† From the Kettering-Meyer Laboratory, Southern Research Institute, Birmingham, Alabama 35255 (C.-H.C., R.W.B., and L.L.B.), and the Division of Biology and Medicine, Brown University, Providence, Rhode Island 02912 (S.C.). *Received July 26, 1982.* This investigation was supported by Grants RO1-CA23155 and RO1-CA31706 awarded by the National Cancer Institute, by Grant SO7-RR-0576 awarded by the Division of Research Resources, Department of Health and Human Services, and by Grant CH-136 from the American Cancer Society.

0006-2960/83/0422-0600$01.50/0 

activity, which interfered with the kinetic and isotope exchange study. Hence, further purification of the enzyme was undertaken. The enzyme preparation obtained from the final step of purification (octyl-Sepharose) described in the previous report (Chang et al., 1980) was further purified by using CM-cellulose column chromatography. Adenosine kinase was not retained on the column and was eluted in a wash with 50 mM Tris-HCl, pH 8.0 (4 °C), 50 μM ethylenediaminetetraacetic acid (EDTA), 1 mM dithiothreitol, 1 mM $MgCl_2$, and 20% sucrose. Adenosine kinase isolated by this means was homogeneous as judged by electrophoretic techniques and was free of NDP kinase activity. All of the studies reported here were performed with enzyme obtained after the CM-cellulose column chromatography. Each experiment was repeated at least 3 times; assays were done in duplicate.

*Isolation of Phosphorylated Adenosine Kinase.* The enzyme was incubated for 5 min at room temperature with [8-$^{14}$C]ATP and/or [γ-$^{32}$P]ATP after which the nucleotides were removed from enzyme either by (a) chromatography on a column of Sephadex G-50 or (b) treatment of the reaction mixture with Norite A (500 μg). Before its use, Norite A was saturated with BSA and then washed with 50 mM Tris buffer, pH 8.0, until BSA was no longer present in the supernatant fluid. Fractions eluted from the column and the total reaction mixture after removal of Norite A were assayed for radioactivity. When both $^{14}$C and $^{32}$P were present, the window of the two channels in the counter was adjusted so that both isotopes could be counted simultaneously. Additional experimental details are given in Table I.

*Isotope Exchange Study.* The enzyme (0.03–0.25 μg) was incubated with [8-$^{14}$C]ADP (0.1–1.0 mM; 8 μCi/mL), 1.25 mM ATP, and 0.4 mM excess $MgCl_2$ either in the presence or absence of 0.5 μM adenosine in a final volume of 0.1 mL. An aliquot (15 μL) of the reaction mixture was spotted on a thin-layer MN-polygram 300 PEI/UV 254 plate previously spotted with a marker composed of a mixture of ADP and ATP. The chromatogram was developed with a solution of 0.5 M LiCl and 2 N acetic acid to a distance of 16 cm. The areas containing ATP and ADP were located under UV light; each area was excised, and the PEI–cellulose was placed in a vial containing 5 mL of scintillation solution for radioactivity determination.

*Phosphorylation of Adenosine by [$^{32}$P]Phosphorylated Adenosine Kinase.* The phosphorylated adenosine kinase, prepared as described under Isolation of Phosphorylated Adenosine Kinase, was incubated with adenosine at 37 °C for 2 h in the presence or absence of $MgCl_2$. The final volume of the enzyme reaction mixture was 0.1 mL. The [$^{32}$P]AMP was isolated by thin-layer chromatography as described under Isotope Exchange Study.

*Protein Determination.* Protein concentrations were determined by the method of Bradford (1976). Bovine serum albumin was used as the standard.

*Calculations.* All statistical analyses were performed by the general methods described by Cleland (1967). These include the least-square fitting of data to straight lines, hyperbolas, or parabolas and computation of standard errors. Whenever applicable, data points were weighted with $n/\sigma^2$ where $\sigma$ is a standard error of estimation.

## Results

*(I) Properties of Adenosine Kinase. (A) Effect of Substrate Concentration on Enzyme Activity.* The effect of adenosine or MgATP in the presence of several fixed concentrations of MgATP or adenosine, respectively, is shown in Figure 1A,B.

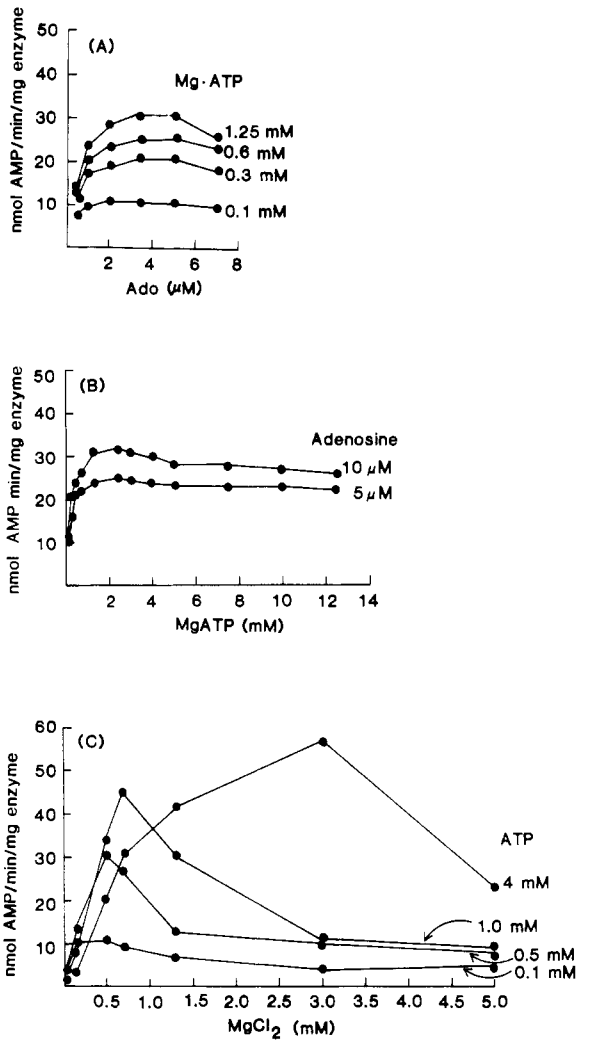


FIGURE 1: Effect of adenosine, MgATP, and $MgCl_2$ on adenosine kinase activity. (A) The effect of adenosine on the enzyme activity with different fixed concentrations of MgATP and with magnesium at a concentration of 0.4 mM in excess of the MgATP concentration. (B) The effect of MgATP on the enzyme activity when adenosine concentration was at 5 and 10 μM and the magnesium was at a concentration of 0.4 mM in excess of the MgATP concentration. (C) The effect of $MgCl_2$ on the enzyme activity with different fixed concentrations of ATP. The concentration of adenosine was 5 μM.

Enzyme activity initially increased with increasing substrate concentrations but decreased at higher concentrations of substrate.

*(B) Effect of Magnesium on Enzyme Activity.* Adenosine kinase from L1210 cells or from human placenta does not phosphorylate adenosine in the absence of magnesium (Chang et al., 1980; Palella et al., 1980). Additional experiments were performed to determine whether MgATP or free ATP was the true substrate for this enzyme. When the concentrations of magnesium were varied at fixed levels of ATP at pH 8.0 (Figure 1C), the peak activity increased as the ATP concentration increased. An increase in $MgCl_2$ concentration to levels well above the optimum for a given adenosine and ATP concentration resulted in inhibition of enzyme activity, in agreement with previous reports (Chang et al., 1980; Palella et al., 1980). In the absence of magnesium, the enzyme does not phosphorylate adenosine at concentrations of ATP ranging from 0.1 to 4 mM (Figure 1C). The decrease in velocity at concentrations of ATP in excess of $MgCl_2$ concentrations suggests that free ATP is inhibitory. It was observed (Chang et al., 1980; Palella et al., 1980) that the pH optimum for

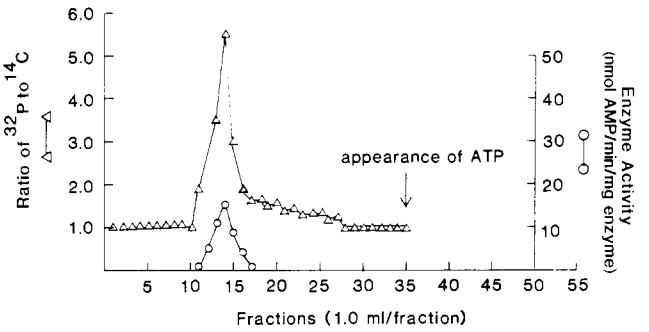


FIGURE 2: Phosphorylation of adenosine kinase. The enzyme (5 μg) was incubated with [8-$^{14}$C]ATP and [γ-$^{32}$P]ATP, as described in Table IA, and loaded on Sephadex G-50 (1.5 × 25 cm) previously equilibrated with 50 mM Tris-HCl, pH 8.0 (4 °C), 50 μM EDTA, 1 mM dithiothreitol, and 20% sucrose. The phosphorylated enzyme was then eluted with the same buffer.

adenosine kinase was a function of the concentration of magnesium and ATP. These observations coupled with the results presented in Figure 1C suggest that the metal–nucleotide complex (MgATP) is the true substrate, in agreement with Palella et al. (1980) and that free ATP or free Mg ion exert inhibitory effects. In order to maintain a high and nearly constant proportion of the ATP in solution as MgATP, a fixed excess of magnesium, 0.4 mM, was used in the initial velocity and product inhibition studies according to Palella et al. (1980).

(*C*) *Phosphorylated Adenosine Kinase.* $^{32}$P was detected in the supernatant fluid when adenosine kinase was incubated with [γ-$^{32}$P]ATP followed by the removal of free [γ-$^{32}$P]ATP by means of adsorption on BSA–charcoal and centrifugation. When the enzyme was treated in the same manner with [8-$^{14}$C]ATP, no $^{14}$C was detected in the supernatant fluid. When it was treated with a mixture of [γ-$^{32}$P]ATP and [8-$^{14}$C]ATP, $^{32}$P, but not $^{14}$C, remained in the supernatant fluid. These results (Table IA) suggest that $^{32}$P was transferred from [$^{32}$P]ATP to the enzyme. Additional evidence for the formation of the phosphorylated enzyme was obtained by chromatography on Sephadex G-50 of the products resulting from incubation of the enzyme with a mixture of [γ-$^{32}$P]ATP and [8-$^{14}$C]ATP (Figure 2). The enzyme activity was separated from ATP and was eluted as a peak with a high $^{32}$P/$^{14}$C ratio. Under the experimental conditions used (Table IA), [$^{32}$P]ATP was the limiting reagent, enzyme protein was present in excess, and BSA and adenosine were not present. Thus, in this experiment, the transfer of 3.6% of $^{32}$P from [$^{32}$P]ATP to enzyme protein was not conducted under optimum conditions and so the results provide qualitative evidence but not quantitative data on the formation of phosphorylated enzyme.

For determination of whether or not the phosphate can be transferred from the phosphorylated protein to adenosine, the experiment described in Table 1B was performed. When $^{32}$P-labeled enzyme (0.003 pmol of $^{32}$P incorporated/pmol of enzyme), prepared as described in Table IA, was incubated with adenosine in the absence of ATP and in the presence or absence of $Mg^{2+}$, there was a transfer of approximately 10% of $^{32}$P from phosphorylated enzyme protein to adenosine (Table IB).

For determination of whether purified enzyme could be phosphorylated by [$^{32}$P]AMP, the enzyme was incubated under the conditions described in Table IA with [$^{32}$P]AMP substituted for [$^{32}$P]ATP. No $^{32}$P was found in the supernatant fluid after removal of the charcoal. Thus, no evidence for reversal of the transfer of $^{32}$P from $^{32}$P-labeled enzyme to adenosine was obtained.

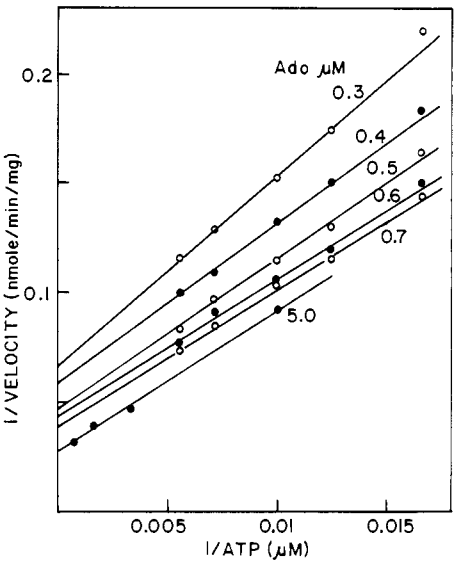


FIGURE 3: Plot of 1/velocity [nmol of AMP formed min$^{-1}$ (mg of enzyme)$^{-1}$] vs. 1/[ATP] (μM) at various concentrations of Ado. $MgCl_2$ was kept at 0.4 mM in excess of ATP.

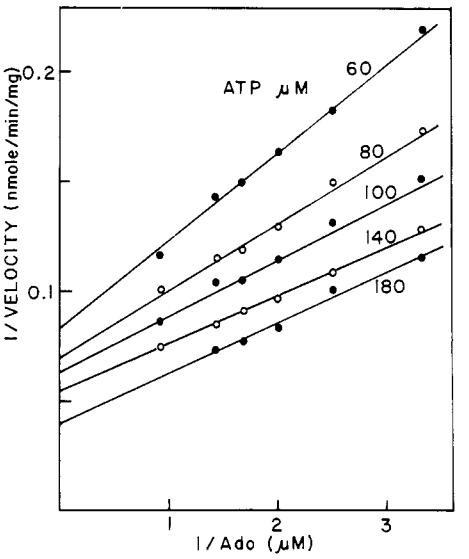


FIGURE 4: Plot of 1/velocity [nmol of AMP formed min$^{-1}$ (mg of enzyme)$^{-1}$] vs. 1/[Ado] (μM) at various concentrations of ATP. $MgCl_2$ was kept at 0.4 mM in excess of ATP.

(*D*) *Isotope Exchange.* The enzyme was incubated for 1 h with [8-$^{14}$C]ADP over a range of concentrations (0–0.7 mM; 0–0.24 μCi/reaction mixture), ATP (1.25 mM), and $Mg^{2+}$ in the absence or presence of adenosine (5 μM) in a final volume of 0.1 mL. Analysis by thin-layer chromatography revealed no formation of [8-$^{14}$C]ATP. Thus, no evidence was obtained for reversibility of the reaction ATP + E → ADP + E∼P.

(*II*) *Kinetic Studies.* The derivation of a rate equation for adenosine kinase is presented in the Appendix. In the following analysis, eq 1–31 refer to equations in this derivation. The meanings of the symbols A, B, E, F, O, P, and Q are given in the legend to Figure 11.

(*A*) *Initial Velocity Studies.* Figures 3 and 4 show the results of initial velocity studies. In each case the differences between slopes were small but statistically significant. Replots of slope, intercept, or apparent $K_m$ vs. 1/[fixed substrate] for the data presented in Figure 3, Figure 4, and those from Figure 1 (double-reciprocal plots not shown) were analyzed in detail according to the rate equation derived in the Appendix.

Table I: Phosphorylation of Adenosine Kinase by ATP and Phosphorylation of Adenosine by the Phosphorylated Kinase

A. Phosphorylation of Adenosine Kinase[a]

| protein added | protein-bound radioactivity (pmol) after incubation with: [8-$^{14}$C]ATP (41 pmol) | [$\gamma$-$^{32}$P]ATP (0.57 pmol) | [8-$^{14}$C]ATP (41 pmol) and [$\gamma$-$^{32}$P]ATP (0.6 pmol): $^{14}$C | $^{32}$P |
|---|---|---|---|---|
| none | 0 | 0 | 0 | 0 |
| BSA | 0 | 0.0007 | 0 | 0.0006 |
| adenosine kinase | 0 | 0.021 | 0 | 0.022 |

B. Phosphorylation of Adenosine by [$^{32}$P]Phosphorylated Adenosine Kinase[b]

| phosphorylated enzyme (pmol of $^{32}$P) | pmol of [$^{32}$P]AMP formed: 1 mM $MgCl_2$ added | no $MgCl_2$ added |
|---|---|---|
| 0 | 0 | 0 |
| 0.0015 | 0.0002 | 0.0002 |
| 0.003 | 0.0003 | 0.0003 |

[a] Each solution (200 $\mu$L final volume) contained [8-$^{14}$C]ATP (210 nM; 0.024 $\mu$Ci) or [$\gamma$-$^{32}$P]ATP (2.9 nM; 0.018 $\mu$Ci). The control contained no added protein; to the other reaction mixtures BSA (36 pmol) or adenosine kinase (7 pmol) was added. All reaction mixtures were incubated for 5 min at room temperature. Norite A (500 $\mu$g) that had been treated with BSA, as described under Experimental Procedures, was added to each reaction mixture. Norite A containing ATP and ADP was removed by centrifugation. The total supernatant solution was added to a scintillation vial containing 5 mL of scintillation solution, and the vial was counted in a Packard Tri-Carb liquid scintillation spectrometer. [b] The phosphorylated enzyme (0.003 pmol of $^{32}$P incorporated/pmol of enzyme), prepared as described in part A, was incubated with adenosine (5 $\mu$M) at 37 °C for 2 h in the presence or absence of $MgCl_2$. The final volume of the enzyme reaction mixture was 0.1 mL. The [$^{32}$P]AMP was isolated by thin-layer chromatography as described in the text and assayed for radioactivity in a liquid scintillation spectrometer.

(*1*) *A as Varied Substrate: Plot of 1/v vs. 1/[ATP].* (*a*) *Replot of Slope vs. 1/[Ado]* (*Figure 5*). The slope ($y$) can be expressed as a function of $x$ ($=1/B$) by substituting $P = Q = O$ and rearranging eq 26 (Appendix).

$$y = \frac{K_{ao}}{E_t}\left[x^2 + \left(\frac{1}{K_{ob}} + \frac{1}{K_{bo}}\right)x + \frac{1}{K_{\bar{b}b}K_{ob}}\right] \Big/ [k_1x^2 + k_2x/K_{a\bar{b}}] \quad (32)$$

It can be shown that the plot of $y$ vs. $x$, i.e., slope against $1/[\text{Ado}]$, can take one of two different shapes depending on certain conditions.

If $k_2/K_{a\bar{b}} < k_1(1/K_{bo} + 1/K_{ob})$, the replot will be a curve having two asymptotes [$x = 0$ and $y = K_{ao}/(k_1E_t)$] and having negative slopes at all values of $x$. Since the data in Figure 5 display a portion of the replot with unmistakably positive slopes, this condition can be ruled out.

If $k_2/K_{a\bar{b}} > k_1(1/K_{bo} + 1/K_{ob})$, on the other hand, the plot should be a curve characterized by (1) $y = \infty$ and $dy/dx < 0$ at $x = 0$, (2) occurrence of a minimum followed by an inflection point, and (3) $y$ asymptotically approaching $K_{ao}/(k_1E_t)$ as $x \rightarrow \infty$. Thus, this curve consists of three parts, as $x$ increases from 0 to $\infty$: (1) a descending part, at a low range of $x$, reflecting the competition of Ado (at high concentrations) with MgATP; (2) an ascending part, at an intermediate range of $x$ where the ternary complex (MgATP·E·Ado) is a significant portion of the enzyme–substrate complexes; (3) a horizontal part at a high range of $x$, i.e., a very low range of Ado where the formation of MgATP·E·Ado complex becomes negligible and MgATP·E is the predominant E–ligand complex.

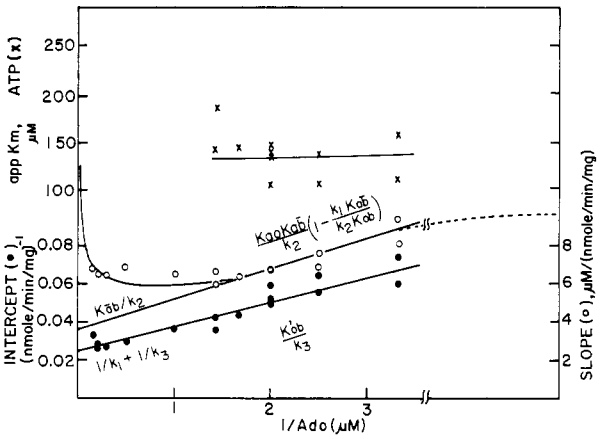


FIGURE 5: Replots of slope (○), intercept (●) of Figure 3, and apparent $K_m$ for [ATP] vs. 1/[Ado] ($\mu$M). Also included in these replots are the parameters estimated for similar double-reciprocal plots (not shown) of the data presented in Figures 1 and 4. The straight lines were fitted to data points by the method of least squares with weight of 1/(standard error)$^2$. The data points for the slopes at the Ado concentrations greater than 1 $\mu$M were not included in the computation of the regression line. The solid and dashed curves are sketches of a curve that might fit to data points if they were available at extremely high or low concentrations of Ado, respectively.

At concentrations of Ado below a certain level (approximately 2 $\mu$M as indicated by Figure 1), the binding of Ado to the MgATP site appears to be insignificant; therefore the terms containing $K_{bo}$ and $K_{\bar{b}b}$ in eq 32 may be eliminated. Then the ascending and horizontal parts of the curve may be represented by a rectangular hyperbola, from which one could, theoretically, estimate the values of various parameters. The available data, however, do not cover a wide enough range of $x$, particularly at the horizontal part of the curve. In such a case, the ascending portion of the curve may be closely approximated by the tangent to the hyperbola at $x = 0$, which is

$$y = \frac{K_{ao}K_{a\bar{b}}}{k_2E_t}\left(1 - \frac{k_1K_{a\bar{b}}}{k_2K_{ob}}\right)x + \frac{K_{\bar{a}b}}{k_2E_t} \quad (33)$$

The values of parameters thus obtained from this ascending part of the curve (Ado range 0.3–1 $\mu$M) are listed in Table II. Note that $E_t = 1$ mg throughout this paper. Since the slope of this replot is positive, $k_1K_{a\bar{b}}/(k_2K_{ob}) < 1$, and since $K_{a\bar{b}}/K_{ob} = K_{\bar{a}b}/K_{ao}$, $k_1/K_{ao} < k_2/K_{\bar{a}b}$. In general, $V_{max}/K_m$ is a measure of substrate efficiency. Hence, it can be concluded that adenosine kinase is phosphorylated by MgATP more efficiently in the presence of bound Ado than in its absence.

(*b*) *Replot of Intercept vs. 1/[Ado]* (*Figure 5*). The intercept ($y$) of the $1/v$ vs. 1/[ATP] plot at various Ado concentrations can be expressed as a function of $x$ ($=1/[\text{Ado}]$) by ignoring the terms accounting for the binding of Ado to the MgATP site, setting $P = Q = O$, and rearranging eq 27 (Appendix):

$$y = \frac{1}{E_t}\left(\frac{K_{a\bar{b}}x + 1}{k_1K_{a\bar{b}}x + k_2}\right) + \frac{K'_{ob}x + 1}{k_3} \quad (34)$$

The plot is a hyperbola with an asymptote represented by

$$y = [K'_{ob}/(k_3E_t)]x + (1/E_t)(1/k_1 + 1/k_3) \quad (35)$$

The $x$ intercept of this asymptote is at

$$x = -(1/K'_{ob})(1 + k_3/k_1) \quad (36)$$

Table II: Experimentally Determined Kinetic Parameters

| line no. | parameter | value[a] | SE[b] | data source |
|---|---|---|---|---|
| 1 | $(K_{ao}K_{a\bar{b}})[1-(k_1/k_2)(K_{a\bar{b}}/K_{ob})]$ | 1.60 | 0.18 | Figure 5, slope vs. $1/B$, slope |
| 2 | $K_{\bar{a}b}/k_2$ | 3.63 | 0.41 | Figure 5, slope vs. $1/B$, intercept |
| 3 | $1/[K_{ob}[1-(k_1/k_2)(K_{a\bar{b}}/K_{ob})]]$ | 2.27 | 0.50 | Figure 5, slope vs. $1/B$, intercept/slope |
| 4 | $K'_{ob}/k_3$ | 0.0118 | 0.0006 | Figure 5, intercept vs. $1/B$, slope |
| 5 | $1/k_1 + 1/k_3$ | 0.025 | 0.0005 | Figure 5, intercept vs. $1/B$, intercept |
| 6 | $(1/K'_{ob})(1+k_3/k_1)$ | 2.12 | 0.12 | Figure 5, intercept vs. $1/B$, intercept/slope |
| 7 | $K_{ao}K_{a\bar{b}}/k_2$ | 1.62 | 0.09 | Figure 6, slope vs. $1/A$, slope |
| 8 | $K_{a\bar{b}}/k_2 + K'_{ob}/k_3$ | 0.0115 | 0.0011 | Figure 6, slope vs. $1/A$, intercept |
| 9 | $(1/K_{ao})[1+(k_2/k_3)(K'_{ob}/K_{a\bar{b}})]$ | 0.0071 | 0.0011 | Figure 6, slope vs. $1/A$, intercept/slope |
| 10 | $K_{\bar{a}b}/k_2$ | 3.36 | 0.21 | Figure 6, intercept vs. $1/A$, slope |
| 11 | $1/k_2 + 1/k_3$ | 0.0218 | 0.0032 | Figure 6, intercept vs. $1/A$, intercept |
| 12 | $(1/K_{\bar{a}b})(1+k_2/k_3)$ | 0.0084 | 0.0012 | Figure 6, intercept vs. $1/A$, intercept/slope |

[a] The units of dissociation constants and first-order rate constants are $\mu$M and nmol min$^{-1}$ mg$^{-1}$, respectively. [b] Standard errors of estimation.

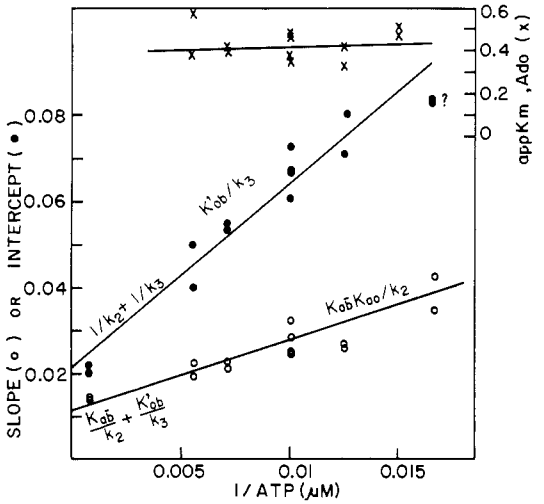


FIGURE 6: Replots of slope (○), intercept (●) of Figure 4, and apparent $K_m$ for [Ado] vs. 1/[ATP] ($\mu$M). Also included in these replots are the parameters estimated from similar double-reciprocal plots (not shown) of the data presented in Figures 1 and 3.

Parameters estimated from the weighted linear regression line through the data points in Figure 5 are listed in Table II.

(*c*) *Apparent* $K_a$ (*Figure 5*). As shown in Figure 5, the values of apparent $K_m$ for ATP do not change significantly at the 0.3–0.7 $\mu$M range of Ado, and the average value is

$$K_a(\text{app}) = 136 \pm 20 \quad (37)$$

As may be seen below, this range of Ado is near the value of $K_{ob}$, and most likely significantly below the value of $K_{a\bar{b}}$. Therefore, this value of $K_a$(app) is an approximate value of $K_{ao}$.

(*2*) *B as Varied Substrate: Plot of* $1/v$ *vs.* $1/[Ado]$. (*a*) *Replot of Slope vs.* $1/[ATP]$ (*Figure 6*). The slope ($y$) can be expressed as a function of $x$ ($=1/A$) by substituting $P = Q = O$ and rearranging eq 29 (Appendix).

$$\text{slope} = \left(\frac{K_{ao}K_{a\bar{b}}}{k_2E_t}\right)x + \left(\frac{K_{a\bar{b}}}{k_2E_t} + \frac{K'_{ob}}{k_3E_t}\right) \quad (38)$$

Parameters estimated from the weighted linear regression line through the data points in Figure 6 are listed in Table II.

(*b*) *Replot of Intercept vs.* $1/[ATP]$ (*Figure 6*). Likewise, the intercept ($y$) as a function of $x$ ($=1/A$) is

$$\text{intercept} = \left(\frac{K_{\bar{a}b}}{k_2E_t}\right)x + \left(\frac{1}{k_2E_t} + \frac{1}{k_3E_t}\right) \quad (39)$$

Parameters estimated from the weighted linear regression line through all but two points at $1/[ATP] = 0.0167$ in Figure 6 are listed in Table II.

(*c*) *Apparent* $K_b$ (*Figure 6*). From eq 38 and 39, apparent $K_m$ for Ado may be expressed as

$$K_b(\text{app}) = K_{ob}\left[K_{\bar{a}b}x + \left(\frac{K_{a\bar{b}}}{K_{ob}} + \frac{k_2K'_{ob}}{k_3K_{ob}}\right)\right] \Big/ [K_{\bar{a}b}x + (1 + k_2/k_3)] \quad (40)$$

As may be seen in Figure 6, the values of apparent $K_b$ appear to vary within a narrow limit at the range of 60–180 $\mu$M ATP. This suggests that the terms in the bracket in the numerator and the denominator must approximately cancel each other. Therefore, within a few-fold error

$$K_{ob} \simeq K_{\bar{a}b} \simeq K'_{ob} \quad (41)$$

This suggests that the effects of phosphorylation of the enzyme and the presence of bound MgATP on the binding of Ado are undetectably small at least over the range of ATP concentrations studied.

(*3*) *Estimation of Kinetic Constants from Initial Velocity Data.* Parameters estimated from Figures 5 and 6 are listed in Table II. Each of these 12 parameters is a combination of some of eight kinetic constants. Since not all of these parameters are independent of each other, and since the experimentally determined values are not accurate enough, it is not feasible to calculate all eight constants. Nevertheless, these data allow computation of some constants and upper and/or lower limits of others. In the following computations, all rate constants ($k$) are expressed in the unit of nmol min$^{-1}$ mg$^{-1}$ and dissociation constants in $\mu$M. Line 2 and line 10 in Table II are two different measures of the same parameter. From the average of these two values

$$K_{\bar{a}b}/k_2 = 3.50 \pm 0.23 \quad (42)$$

From this value and line 7

$$K_{ob} = K_{ao}K_{a\bar{b}}/K_{\bar{a}b} = 0.46 \pm 0.04 \quad (43)$$

Since it appears that Ado binds to the free enzyme and to the phosphorylated enzyme with approximately the same affinity (eq 41), $K_{ob} \simeq K'_{ob}$. Therefore, from line 4, $k_3 \simeq 40$ nmol min$^{-1}$ mg$^{-1}$. Given this approximate value of $k_3$, line 5 and line 11 indicate that both $1/k_1$ and $1/k_2$ must be smaller than the magnitude of the experimental error of the $1/k_3$ value. Thus from line 5 and line 11

$$k_3 \simeq 45.9 \pm 6.7 \quad (44)$$

$$k_1 \gg k_3 \quad (45)$$

$$k_2 \gg k_3 \quad (46)$$

When line 4 is multiplied by the value of $k_3$

$$K'_{ob} \simeq 0.540 \pm 0.085 \quad (47)$$

From this value and line 6

$$k_1/k_3 = 6.8 \pm 1.8 \quad (48)$$

This ratio of $k_1/k_3$ indicates that the formation of AMP from E~P and Ado is the rate-limiting step. Calculation of $k_1$ from this ratio and from the value of $k_3$ gives $k_1 = 313 \pm 1152$. Because of the large standard error, however, this value is meaningless. Now since $k_2 \gg k_3$ also appears to be valid, from line 9 and eq 41

$$K_{ao} \gg 140 \pm 22 \quad (49)$$

This value of $K_{ao}$ may be compared with that of $K_a$(app) (136 ± 20 μM, eq 37). Also from line 10

$$K_{\bar{a}b} = 3.86(\pm 0.21)k_2 \gg 3.36(\pm 0.21)k_3 = 154 \pm 24 \quad (50)$$

From the values of $K_{ao}$, $K_{\bar{a}b}$, and $K_{ob}$

$$K_{a\bar{b}} = K_{ob}K_{\bar{a}b}/K_{ao} \simeq 0.51 \pm 0.12 \quad (51)$$

These estimated values of various parameters are listed in Table III. It should be noted that the standard errors listed in Tables II and III are measures of precision that account for random experimental variation but are not measures of accuracy, because errors introduced by the various approximations used during the derivation of rate equations cannot be accounted for. Therefore, all values calculated above should be understood as approximations. Furthermore, a possible source of error in interpreting kinetic data could rise from the fact that the degree of inhibition by free magnesium ions depends on the actual concentration of MgATP. However, it appears that this was not a significant factor, at least in the range of ATP concentrations studied, since the plots of $1/v$ vs. $1/[ATP]$ (e.g., Figure 3) were all linear.

(*B*) *Product Inhibition Studies.* The results of various product inhibition studies are presented in Figures 7-10 and summarized in Table IV. Interpretations of these data and estimations of various parameters thereof are as follows.

(*1*) *ATP Varied and ADP as Inhibitor* (*Figure 7*). The parameters of the plot of $1/v$ vs. $1/A$ in eq 26 and 27 (Appendix) at $P > O$ and $Q = O$ may be rearranged to

$$\text{slope} = \frac{K_{ao}}{E_t}\left[\left(1 + \frac{B}{K_{ob}} + \frac{B}{K_{bo}} + \frac{B^2}{K_{ob}K_{\bar{b}b}}\right)\Big/\left(k_1 + \frac{k_2B}{K_{a\bar{b}}}\right) + \frac{P}{K_{po}}\left[\left(1 + \frac{B}{K_{p\bar{b}}}\right)\Big/\left(k_1 + \frac{k_2B}{K_{a\bar{b}}}\right)\right]\right] \quad (52)$$

$$\text{intercept} = \frac{1}{E_t}\left[\left(1 + \frac{B}{K_{\bar{a}b}}\right)\Big/\left(k_1 + \frac{k_2B}{K_{a\bar{b}}}\right) + \left[1 + \frac{B}{K'_{ob}} + \frac{B}{K'_{bo}} + \frac{B^2}{K'_{ob}K'_{\bar{b}b}} + \frac{P}{K'_{po}}\left(1 + \frac{B}{K'_{p\bar{b}}}\right)\right]\Big/\left[\frac{B}{K'_{ob}}\left(k_3 + \frac{k_4P}{K'_{po}} + \frac{k_6B}{K'_{\bar{b}b}}\right)\right]\right] \quad (53)$$

These parameters indicate that, in general, an S-linear I-hyperbolic noncompetitive inhibition pattern should be seen.

The replot of slope vs. [ADP] should be a straight line, and the data in Figure 7 (inset a) are consistent with this prediction.

Table III: Kinetic Constants

| parameters | reactions | values[a] | SE[b] |
|---|---|---|---|
| $K_{ao}$ | MgATP·E → E + MgATP | >140 | 22 |
| $K_{\bar{a}b}$ | MgATP·E·Ado → E·Ado + MgATP | >154 | 24 |
| $K_{ob}$ | E·Ado → E + Ado | 0.46 | 0.04 |
| $K_{a\bar{b}}$ | MgATP·E·Ado → MgATP·E + Ado | 0.51 | 0.12 |
| $K'_{ob}$ | E~P·Ado → E~P + Ado | 0.54 | 0.09 |
| $K_{po}$ | MgADP·E → E + MgADP | 92.4 | 11.4 |
| $K'_{po}$ | MgADP·E → E~P + MgADP | >>$K_{po}$ | |
| $K_{\bar{p}b}$ | MgADP·E·Ado → E·Ado + MgADP | <118 | 13 |
| $K_{oq}$ | E·AMP → E + AMP | <253 | 31 |
| $K_{qo}$ | AMP·E → E + AMP | >>$K_{oq}$ | |
| $K'_{qo}$ | AMP·E~P → E~P + AMP | ≃629 | 16 |
| $K_{q\bar{q}}$ | AMP·E·AMP → AMP·E + AMP | <<$K_{\bar{q}q}$ | |
| $K_{\bar{q}q}$ | AMP·E·AMP → E·AMP + AMP | <2045 | 364 |
| $k_1$ | MgATP·E → MgADP·E~P | >$k_3$ | |
| $k_2$ | MgATP·E·Ado → MgADP·E~P·Ado | >$k_3$ | |
| $k_3$ | E~P·Ado → E·AMP | 45.9 | 6.7 |
| $k_4$ | MgADP·E~P·Ado → MgADP·E·AMP | <<$k_3$ | |
| $k_5$ | AMP·E~P·Ado → AMP·E·AMP | <<$k_3$ | |
| $k_6$ | Ado·E~P·Ado → Ado·E·AMP | ?<<$k_3$ | |

[a] The units of dissociation constants and first-order rate constants are μM and nmol $min^{-1}$ $mg^{-1}$, respectively. [b] Standard errors of estimation.

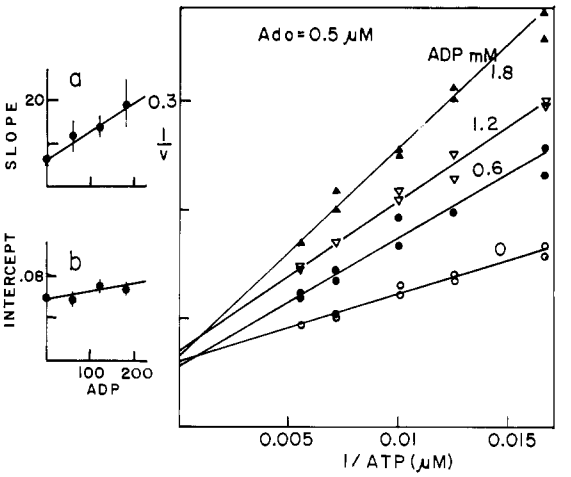


FIGURE 7: Plot of $1/v$ vs. $1/[ATP]$ at various concentrations of the product inhibitor ADP at a level of Ado fixed at 0.5 μM. $MgCl_2$ was kept at 0.4 mM in excess of [ATP] plus [ADP]. The perpendicular lines indicate standard errors of estimation of parameters.

The apparent $K_p$ evaluated from the $x$ intercept of the replot according to eq 52 is

$$K_{is} = K_p(\text{app}) = K_{po}\left(1 + \frac{B}{K_{ob}} + \frac{B}{K_{bo}} + \frac{B^2}{K_{ob}K_{\bar{b}b}}\right)\Big/\left(1 + \frac{B}{K_{p\bar{b}}}\right) \quad (54)$$

Since there is no significant difference between two values of $K_{is}$ at two widely different concentrations of Ado (Table IV), the term in the parenthesis in the numerator and the denominator of the above equation must approximately cancel each other so that $K_{is}$ is indeed an approximate value of $K_{po}$. Thus, taking the average of the two $K_{is}$ values

$$K_{po} \simeq 92.4 \pm 11.4 \quad (55)$$

On the other hand, the replot of intercept vs. ADP should be a rectangular hyperbola unless $k_4 = 0$. Although the number of points in the inset b of Figure 7 is inadequate to distinguish between a straight line and a hyperbola, other

Table IV: Apparent Inhibition Constants ($\mu$M)[a]

| | MgATP varied (60–80 $\mu$M) | | | | | | Ado varied (0.3–0.7 $\mu$M) | | | | | |
|---|---|---|---|---|---|---|---|---|---|---|---|---|
| | Ado = 5 $\mu$M | | | Ado = 0.5 $\mu$M | | | MgATP = 1250 $\mu$M | | | MgATP = 100 $\mu$M | | |
| product inhibitor | figure | $K_{is}$ ± SE | $K_{ii}$ ± SE | figure | $K_{is}$ ± SE | $K_{ii}$ ± SE | figure | $K_{is}$ ± SE | $K_{ii}$ ± SE | figure | $K_{is}$ ± SE | $K_{ii}$ ± SE |
| ADP (0–180 $\mu$M) | 7[b] | 88.0 ± 1.5 | 279 ± 67 | 7 | 96.7 ± 11.3 | 938 ± 523 | | | | 9 | 240 ± 32 | 118 ± 13 |
| ADP (0–1800 $\mu$M) | | | | | | | 9[b] | 272 ± 85 | 513 ± 100 | | | |
| AMP (0–1800 $\mu$M) | | | | 8[b] | 576 ± 35 | 629 ± 16 | 10[b] | 519 ± 16 | 730 ± 217 | 10 | 253 ± 31 | $\infty$ |
| AMP (0–10000 $\mu$M) | 8 | parabolic | 787 ± 178 | | | | | | | | | |

[a] $K_{is}$ and $K_{ii}$ are the apparent $K_i$ estimated from the slope and intercept of a double-reciprocal plot of $1/v$ vs. $1/S$, respectively. The units of all inhibition constants are expressed in $\mu$M. [b] Figure not shown.

product inhibition studies analyzed below indicate that both $k_4$ and $k_6$ are negligibly small compared to $k_3$. In addition it has been established that $k_2 \gg k_3$ (eq 46). When all these conditions are taken into consideration, it can be shown that $k_{ii}$ is an approximate measure of $K'_{po}$ and it is relatively independent of the Ado concentration employed. Although the two $K_{ii}$ values estimated at Ado concentrations of 0.5 and 5 $\mu$M appear to be different, this difference is statistically insignificant because of the large standard errors of estimation. Therefore, an accurate estimation of $K'_{po}$ on the basis of these data is not feasible. Nevertheless, from the data in Figure 7 and the above arguments it may be concluded that

$$K_{ii} \simeq K'_{po} \gg K_{po} \tag{56}$$

The implication of this conclusion is that MgADP binds much less tightly to E~P than to E. Since the diffusion-controlled rates of association of MgADP are expected to be approximately the same regardless of whether it binds to E~P or E, this difference must be accounted for by the difference in the rate of dissociation. Then it follows that, after the transfer of the phosphoryl group of ATP to the enzyme, the product MgADP must dissociate very rapidly from the phosphorylated enzyme, most likely before the formation of AMP. Then the second half of the reaction pathway, in all practical sense, would be an ordered sequence, with AMP being the last product to dissociate.

(2) *ATP Varied: AMP as Inhibitor (Figure 8).* The parameters of the $1/v$ vs. $1/A$ plot in eq 26 and eq 27 (Appendix) at $P = O$ and $Q > O$ may be rearranged to

$$\text{slope} = \left[K_{ao}\Big/\left[E_t\left(k_1 + \frac{k_2 B}{K_{a\bar{b}}}\right)\right]\right]\left[1 + \frac{B}{K_{ob}} + \frac{B}{K_{bo}} + \frac{B^2}{K_{ob}K_{\bar{b}b}} + \frac{Q}{K_{oq}}\left(1 + \frac{B}{K_{\bar{b}q}}\right) + \frac{Q}{K_{qo}}\left(1 + \frac{B}{K_{q\bar{b}}}\right) + \frac{Q^2}{K_{oq}K_{\bar{q}q}}\right] \tag{57}$$

$$\text{intercept} = \frac{1}{E_t}\left[\left(1 + \frac{B}{K_{a\bar{b}}}\right)\Big/\left(k_1 + \frac{k_2 B}{K_{a\bar{b}}}\right) + \left[1 + \frac{B}{K'_{ob}} + \frac{B}{K'_{bo}} + \frac{B^2}{K'_{ob}K'_{\bar{b}b}} + \frac{Q}{K'_{qo}}\left(1 + \frac{B}{K'_{q\bar{b}}}\right)\right]\Big/\left[\frac{B}{K'_{ob}}\left(k_3 + \frac{k_5 Q}{K'_{\bar{q}b}} + \frac{k_6 B}{K'_{\bar{b}b}}\right)\right]\right] \tag{58}$$

Equation 57 predicts that, at a high range of $A$ where $Q/K_{\bar{q}q}$ is significant, the replot of slope vs. $Q$ should be a parabola, whereas at a low range of $Q$, it should approach a straight line. The data are consistent with these predictions. The data in inset a of Figure 8 fit more closely to a parabola than to a straight line, i.e.

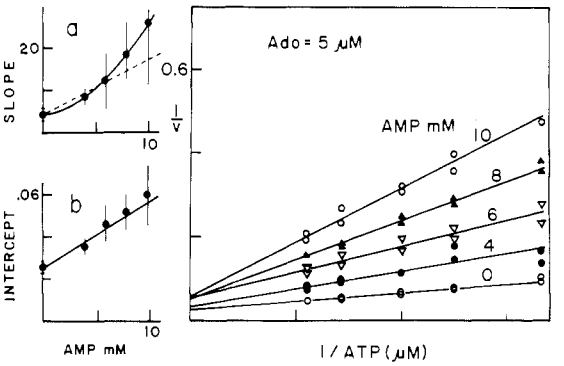


FIGURE 8: Plot of $1/v$ vs. $1/[ATP]$ at various concentrations of the product inhibitor AMP at a level of Ado fixed at 5 $\mu$M. $MgCl_2$ was kept at 0.4 mM in excess of ATP. Inset a shows that the replot of slope vs. AMP fits better to a parabola (solid line) than to a straight line (dashed line).

$$y = a + bQ + cQ^2 \tag{59}$$

where $a = 4.12 \pm 0.045$, $b = 0.364\ (\pm 0.049) \times 10^{-3}$, and $c = 0.178\ (\pm 0.008) \times 10^{-6}$.

Then, from eq 57 it can be shown that

$$b/c = K_{q\bar{q}}\left(1 + \frac{B}{K_{q\bar{b}}}\right) + K_{\bar{q}q}\left(1 + \frac{B}{K_{\bar{b}q}}\right) = 2045 \pm 364 \tag{60}$$

Therefore

$$K_{q\bar{q}} + K_{\bar{q}q} < 2045 \pm 364 \tag{61}$$

When lower concentration ranges of both Ado (0.5 $\mu$M) and AMP (0–1.5 mM) were employed, however, both replots of slope vs. $Q$ and intercept vs. $Q$ were linear (data summarized in Table IV). This fact can be explained as follows. When the range of $Q$ is low the $Q^2$ term in eq 59 becomes negligible; thus the replot of slope vs. $Q$ becomes linear and $K_{is} = a/b$.

$$K_{is} = a/b = K_{oq}K_{qo}\left(1 + \frac{B}{K_{ob}} + \frac{B}{K_{bo}} + \frac{B^2}{K_{ob}K_{\bar{b}b}}\right)\Big/\left[K_{qo}\left(1 + \frac{B}{K_{\bar{b}q}}\right) + K_{oq}\left(1 + \frac{B}{K_{q\bar{b}}}\right)\right] \tag{62}$$

The values of $a/b$ at two concentrations of B (5 and 0.5 $\mu$M) are 11320 ± 1530 and 576 ± 35 $\mu$M, respectively. Since $K_{is}$ decreases as $B$ decreases, extrapolating to $B = 0$

$$K_{oq}K_{qo}/(K_{oq} + K_{qo}) < 576 \pm 35 \tag{63}$$

The replot of intercept vs. [AMP] should be a rectangular hyperbola according to eq 58. The data, however, indicate that the plot is a straight line at the very high (Figure 8) and

low (<1.5 mM) concentration ranges of Q. Therefore, it may be concluded that $k_5 \ll (k_3 + k_6B/K'_{\bar{b}b})$, or that

$$k_5 \simeq 0 \tag{64}$$

This means that the transphosphorylation from E~P to Ado in the presence of AMP at the MgATP site proceeds at a negligibly small rate, if at all. The value of $K_{ii}$ at the low Ado concentration (0.5 $\mu$M) may be considered as a fair approximation of $K'_{qo}$; thus

$$K'_{qo} \simeq 629 \pm 16 \tag{65}$$

*(3) Ado Varied and ADP as Inhibitor (Figure 9).* The parameters of the plot of $1/v$ vs. $1/B$ in eq 29 and eq 30 at $P > 0$ and $Q = 0$ may be rearranged to

$$\text{slope} = \frac{K_{a\bar{b}}}{k_2E_t}\left[1 + \frac{k_2K'_{ob}}{K_{a\bar{b}}}\Big/\left(k_3 + \frac{k_4P}{K'_{\bar{p}b}}\right) + \frac{K_{ao}}{A} + \frac{P}{K_{po}}\left[\frac{k_2K'_{ob}K_{po}}{K_{a\bar{b}}K'_{po}}\Big/\left(k_3 + \frac{k_4P}{K'_{\bar{p}b}}\right) + \frac{K_{ao}}{A}\right]\right] \tag{66}$$

$$\text{intercept} = \frac{1}{k_2E_t}\left[1 + k_2\Big/\left(k_3 + \frac{k_4P}{K'_{\bar{p}b}}\right) + \frac{K_{\bar{a}b}}{A} + \frac{P}{K_{\bar{p}b}}\left[\frac{k_2K_{\bar{p}b}}{K'_{\bar{p}b}}\Big/\left(k_3 + \frac{k_4P}{K'_{\bar{p}b}}\right) + \frac{K_{\bar{a}b}}{A}\right]\right] \tag{67}$$

These equations indicate that, in general, replots of both slope vs. ADP and intercept vs. ADP should be hyperbolas. However, the plots of actual data are unmistakably straight lines, indicating that either $P/K'_{\bar{p}b} \ll 1$ and/or $k_4 \ll k_3$. Since the initial velocity studies indicated that neither $k_1$ nor $k_2$ is zero, both enzyme species PFO and PFB must occur. Therefore, it is logical to conclude that $k_4$, the rate of conversion of PFB (i.e., MgADP·E~P·Ado) complex to PEQ, is negligibly small, again suggesting that MgADP dissociates before the formation of AMP.

$$k_4 \simeq 0 \tag{68}$$

After terms containing $k_4$ are eliminated in the above two equations, $k_{is}$ and $k_{ii}$ become

$$K_{is} = K_{po}\left[1 + \frac{A}{K_{ao}}\left(1 + \frac{k_2K'_{ob}}{k_3K_{a\bar{b}}}\right)\right]\Big/\left[1 + \frac{A}{K_{ao}}\left(\frac{k_2K'_{ob}K_{po}}{k_3K_{a\bar{b}}K'_{po}}\right)\right] \tag{69}$$

$$K_{ii} = K_{\bar{p}b}\left[1 + \frac{A}{K_{\bar{a}b}}\left(1 + \frac{k_2}{k_3}\right)\right]\Big/\left[1 + \frac{A}{K_{\bar{a}b}}\left(\frac{k_2K_{\bar{p}b}}{k_3K'_{\bar{p}b}}\right)\right] \tag{70}$$

These equations indicate that $K_{is}$ and $K_{ii}$ are the limiting values of $K_{po}$ and $K_{\bar{p}b}$, respectively, as $A$ approaches 0. The fact that the values of both $K_{is}$ and $K_{ii}$ increase as $A$ increases (Table IV) is consistent with these equations. In the absence of data for a wider range of $A$, however, $K_{is}$ and $K_{ii}$ provide only upper limits of $K_{po}$ and $K_{\bar{p}b}$, respectively.

$$K_{po} < 240 \pm 32 \tag{71}$$

$$K_{\bar{p}b} < 118 \pm 13 \tag{72}$$

This upper limit of $K_{po}$ is comparable to the value (92.4 ± 11.4 $\mu$M) already estimated (eq 55). Thus it appears that $K_{po} \simeq K_{\bar{p}b}$, i.e., the binding of MgADP to the MgATP site, is not significantly affected by the presence of Ado at the Ado site.

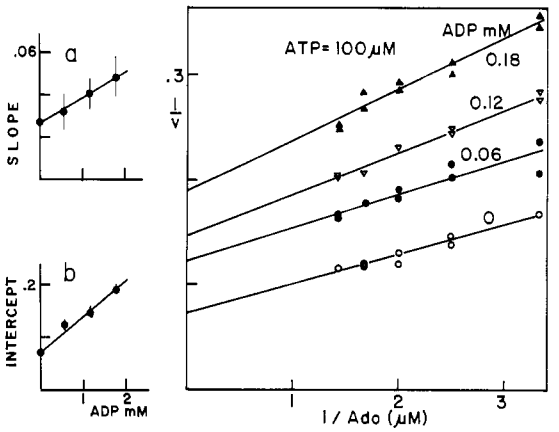


FIGURE 9: Plot of $1/v$ vs. $1/[\text{Ado}]$ ($\mu$M) at various concentrations of the product inhibitor ADP and a level of ATP fixed at 100 $\mu$M. $MgCl_2$ was kept at 0.4 mM in excess of [ATP] plus [ADP].

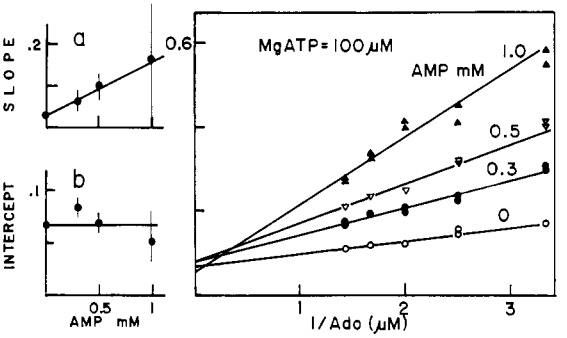


FIGURE 10: Plot of $1/v$ vs. $1/[\text{Ado}]$ ($\mu$M) at various concentrations of the product inhibitor AMP and a level of ATP fixed at 100 $\mu$M.

There is another factor that must be considered in the interpretation of kinetic experiments where ADP was added. Since the total $Mg^{2+}$ was kept at 0.4 mM in excess of [ATP] + [ADP], and because ADP binds $Mg^{2+}$ less tightly, free magnesium ion concentrations would have been higher in a solution containing ADP than in one without ADP. Thus, both the actual concentration of free $Mg^{2+}$ and the ratio of $[\text{ADP}]/[Mg^{2+}]$ would be different depending on ADP concentration. Had the difference in free $Mg^{2+}$ concentration made a significant contribution to inhibition under these conditions, one or both replots of slope vs. ADP and intercept vs. ADP would have been nonlinear. The fact that the replots of both Figures 7 and 9, as well as others not shown but summarized in Table IV were all straight lines indicates that the effect of difference in free $Mg^{2+}$ due to different ADP concentration was negligibly small in the range of ADP concentrations employed.

*(4) Ado Varied: AMP as Inhibitor (Figure 10).* The parameters of the $1/v$ vs. $1/B$ plot in eq 29 and eq 30 at $P = 0$, $Q > 0$, and $k_5 = 0$ may be rearranged to

$$\text{slope} = \frac{K_{a\bar{b}}}{k_2E_t}\left[\left(1 + \frac{k_2K'_{ob}}{k_3K_{a\bar{b}}} + \frac{K_{ao}}{A}\right) + \frac{Q}{K_{oq}}\left(\frac{k_2K'_{ob}K_{oq}}{k_3K_{a\bar{b}}K'_{qo}} + \frac{K_{ao}}{A}\left(1 + \frac{K_{oq}}{K_{qo}} + \frac{Q}{K_{\bar{q}q}}\right)\right)\right] \tag{73}$$

$$\text{intercept} = \frac{1}{k_2E_t}\left[1 + \frac{k_2}{k_3} + \frac{K_{\bar{a}b}}{A} + \frac{Q}{K_{\bar{q}b}}\left(\frac{k_2K_{\bar{q}b}}{k_3K'_{\bar{q}b}} + \frac{K_{\bar{a}b}}{A}\right)\right] \tag{74}$$

Since the intercept is independent of $Q$ even at a low concentration of A and since the slope is linear with respect to

Scheme I

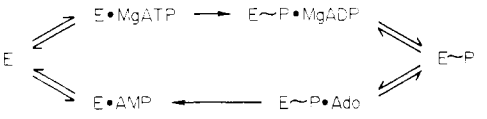


$Q$, the terms containing $K_{qo}$, $K_{\bar{q}b}$, $K_{\bar{q}q}$, and $K'_{\bar{q}b}$, i.e., the binding of AMP to the MgATP site, is insignificant at the concentration range of AMP employed (<1.8 mM). It has already been established that $k_5$ is negligible (eq 64). After all negligible terms are eliminated from the above two equations, the expression of $K_{is}$ becomes

$$K_{is} = K_{oq}\left[1 + \frac{A}{K_{ao}}\left(1 + \frac{k_2 K'_{ob}}{k_3 K_{a\bar{b}}}\right)\right] \quad (75)$$

When the two sets of values of $K_{is}$ and $A$ ($K_{is} = 253 \pm 31$ at $A = 100$ and $K_{is} = 519 \pm 16$ at $A = 1250$) are extrapolated to $A = 0$, the limiting value of $K_{is}$ becomes

$$K_{oq} < 253 \pm 31 \quad (76)$$

If concentrations of AMP substantially higher than the values of $K_{qo}$ were employed, one would expect to observe a parabola on the replot of slope vs. [AMP]. On the other hand, eq 74 indicates that, at the lower range of $Q$ where $Q/K'_{\bar{q}b}$ is negligible, the intercept should be independent of $Q$, i.e., AMP should behave like a competitive inhibitor with respect to Ado. The experimental data, i.e., $K_{ij} = \infty$ when MgATP = 100 $\mu$M and Ado $\leq$ 1 $\mu$M (see Table IV), agree with this prediction.

From eq 63 and eq 76, it can be concluded that

$$K_{qo} \gg K_{oq} \quad (77)$$

and from eq 13 and eq 77

$$K_{\bar{q}q} \gg K_{q\bar{q}} \quad (78)$$

These two relationships indicate that the affinity of AMP toward the MgATP site is much smaller than that for the Ado site.

## Discussion

The isolation of the phosphorylated enzyme (Table I and Figure 2) and the demonstration of formation of AMP from the phosphorylated enzyme and adenosine strongly suggest that the reaction of adenosine kinase might follow the ping-pong mechanism depicted in Scheme I.

The kinetic data, however, do not agree with this simple ping-pong mechanism. Instead of the expected parallel lines, double-reciprocal plots of initial velocity studies (Figures 3 and 4) show definitely different slopes. Moreover, nonlinear replots of slope vs. the reciprocal of substrate and slope vs. inhibitor are seen in an initial velocity study (Figure 5) and in a product inhibition study (Figure 8). These facts indicate that, instead of a single binding site for both substrates, as implied in the classical ping-pong mechanism model, there may be two substrate binding sites, one for MgATP and the other for Ado, which may be occupied simultaneously. Furthermore, the substrate inhibition by Ado shown in Figure 1A could result from the binding of Ado to the MgATP site in competition with MgATP with the resultant formation of an abortive E–Ado complex. For these reasons, we propose a version of the hybrid (or two-site) ping-pong mechanism (Segal, 1975; Northrop, 1969; Cleland, 1973). This is presented in Figure 11.

The data in Figure 1B suggest a possible occurrence of BEA (Ado•E•MgATP) and/or OFA (E~P•MgATP) (see Figure 11). However, the effects of these species are realized only at very high concentrations of MgATP. Hence, the abortive

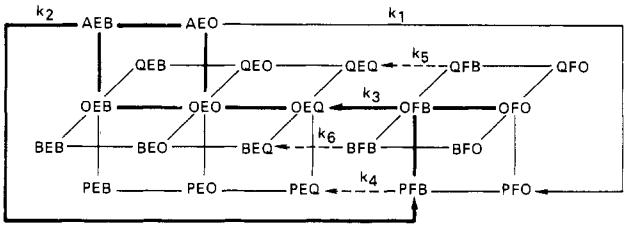


FIGURE 11: Scheme for the reaction catalyzed by adenosine kinase. E and F represent the nonphosphorylated and phosphorylated forms of the enzyme, respectively; the letters A, B, P, and Q represent MgATP, Ado, MgADP, and AMP, respectively; a letter on the left and the right of E or F represents a ligand bound to the MgATP site or the Ado site, respectively; the letter O represents an unoccupied site; $k$ with a subscript number represents the first-order rate constant pertaining to the isomerization of the appropriate enzyme–ligand complex. Note that conceivable enzyme species which could result from the binding of MgATP or MgADP on the Ado site, e.g., BFA and QFP, are not included in the figure in order to avoid undue complexity. The bold lines represent what appear to be the predominant routes of the reaction, and the dashed lines designate the steps that proceed at negligibly slow rates (if at all).

binding of these ligands to the Ado site is ignored. In addition, the species AEQ is omitted from the scheme, since, in order for the ternary complex MgATP•E•AMP to occur, one phosphoryl group, either from ATP or AMP, must be "dangling out" from the enzyme surface. If this unlikely event were to occur, the binding might be much less tight than that of "snuggly fitting" complexes. Actual transphosphorylation steps are considered irreversible since the ATP–ADP exchange reaction does not take place and the enzyme cannot be phosphorylated by AMP. The predominant route of the reaction appears to be that designated by the bold lines in Figure 11, as deduced in the analyses of data.

The results of substrate binding studies, isotope exchange studies, and kinetic studies are consistent in every detail with a two-site ping-pong mechanism as proposed in Figure 11. Furthermore, it became evident that the relative magnitudes of various kinetic constants are such that the predominant pathway appears to be a random binding of two substrates to form the ternary complex MgATP•E•Ado followed by transphosphorylation to form MgADP•E~P•Ado, dissociation of MgADP, the second transphosphorylation to form E•AMP, and finally dissociation of AMP.

Nevertheless, the fact that the phosphorylated enzyme can serve as an intermediate does not rule out the possibility that the phosphoryl group of ATP may be directly transferred to Ado by a concerted mechanism. Indeed, two different versions of an ordered bi-bi mechanism have been proposed in the literature for adenosine kinase albeit from different sources, Ehrlich ascites cells (Henderson et al., 1972) and human placenta (Palella et al., 1980). Therefore, it would be prudent to examine those alternative possibilities. Rate equations have been derived and tested against most other possibilities, including random mechanisms, with equal scrutiny as for the two-site ping-pong mechanism. The results showed that none of those sequential mechanisms are completely consistent with the observed data.

Therefore, we conclude the following: (1) that the two-site ping-pong reaction pathway with the phosphorylated enzyme as an obligatory intermediate is the most likely mechanism of adenosine kinase from L1210 cells; (2) that, among many possibilities within the mechanism, the preferred route is the random binding of substrates followed by a sequential dissociation of MgADP and AMP; (3) that MgATP and Ado decrease the affinity of each other for their respective binding sites; (4) that phosphorylation of the enzyme by MgATP is

irreversible and proceeds more rapidly in the presence of bound Ado; (5) that the stimulatory effect of Ado on the phosphorylation of the enzyme by MgATP is greater than the inhibitory effect of Ado on the binding of MgATP; (6) that the transphosphorylation from the enzyme to Ado proceeds very slowly, if at all, when a ligand is bound to the MgATP site; (7) that the product MgADP dissociates rapidly from the phosphorylated enzyme; and (8) that the formation of AMP from the phosphorylated enzyme and Ado is the rate-limiting step in the entire sequence and does not require any metal ion.

Acknowledgments

We are indebted to Dr. Fardos N. M. Naguib for her critical reading of the manuscript including verification of mathematical derivations. We also thank Mary Trader and Maxie Witt, Chemotherapy Department, for passage of L1210 ascites tumor cells and Nancy DuBois, Biochemistry Department, for technical assistance in harvesting and preparing L1210 leukemia cells. We extend especial thanks to Reta Sisk for preparation of the manuscript in its final form.

## Appendix: Derivation of Rate Equation

Under the assumptions that the association and dissociation of ligands to and from E or F are in random order and that these processes occur more rapidly than the transphosphorylation reactions, a rate equation may be derived by using the previously published method (Cha, 1968). In this method, all nonphosphorylated enzyme species are considered to belong to the equilibrium segment $\sum$E and all the phosphorylated enzyme species to the equilibrium segment $\sum$F. Under these conditions, the reaction mechanism may be represented by Scheme II.

Scheme II

$$\sum \mathrm{E} \underset{k_3f_3 + k_4f_4 + k_5f_5 + k_6f_6}{\overset{k_1f_1 + k_2f_2}{\rightleftharpoons}} \sum \mathrm{F}$$

In this scheme, a subscripted symbol f represents the fraction of an equilibrium segment ($\sum$E or $\sum$F) which exists as a particular enzyme species at overall steady-state conditions. $K$ and $K'$ with appropriate subscripts are dissociation constants of various E– and F–ligand complexes, respectively; the first and second subscripts represent the ligands (o if unoccupied) on the MgATP site and the Ado site, respectively, and a bar above the subscript identifies the species of ligand that dissociates. For example $K_{b\bar{b}}$ is the dissociation constant for BEB → BEO + B, and $K'_{\bar{q}b}$ is that for QFB → OFB + Q. Thus

$$f_1 = (\mathrm{AEO})/\sum E = (A/K_{ao})/\sum_e \quad (1)$$

$$f_2 = (\mathrm{AEB})/\sum E = (A/K_{ao})(B/K_{a\bar{b}})/\sum_e \quad (2)$$

$$f_3 = (\mathrm{OFB})/\sum F = (B/K'_{ob})/\sum_f \quad (3)$$

$$f_4 = (\mathrm{PFB})/\sum F = (B/K'_{ob})(P/K'_{\bar{p}b})/\sum_f \quad (4)$$

$$f_5 = (\mathrm{QFB})/\sum F = (B/K'_{ob})(Q/K'_{\bar{q}b})/\sum_f \quad (5)$$

$$f_6 = (\mathrm{BFB})/\sum F = (B/K'_{ob})(B/K'_{\bar{b}b})/\sum_f \quad (6)$$

where

$$\sum_e = \left(1 + \frac{A}{K_{ao}} + \frac{P}{K_{po}} + \frac{Q}{K_{qo}} + \frac{B}{K_{bo}}\right) + \frac{B}{K_{ob}}\left(1 + \frac{A}{K_{\bar{a}b}} + \frac{P}{K_{\bar{p}b}} + \frac{Q}{K_{\bar{q}b}} + \frac{B}{K_{\bar{b}b}}\right) + \frac{Q}{K_{oq}}\left(1 + \frac{P}{K_{\bar{p}q}} + \frac{Q}{K_{\bar{q}q}} + \frac{B}{K_{\bar{b}q}}\right) \quad (7)$$

$$\sum_f = \left(1 + \frac{P}{K'_{po}} + \frac{Q}{K'_{qo}} + \frac{B}{K'_{bo}}\right) + \frac{B}{K'_{ob}}\left(1 + \frac{P}{K'_{\bar{p}b}} + \frac{Q}{K'_{\bar{q}b}} + \frac{B}{K'_{\bar{b}b}}\right) \quad (8)$$

For each of ten ternary complexes, an identity relationship holds among four dissociation constants.

$$K_{ao}K_{a\bar{b}} = K_{ob}K_{\bar{a}b} \quad (9)$$

$$K_{ob}K_{\bar{p}b} = K_{po}K_{p\bar{b}} \quad (10)$$

$$K_{ob}K_{\bar{q}b} = K_{qo}K_{q\bar{b}} \quad (11)$$

$$K_{ob}K_{\bar{b}b} = K_{bo}K_{b\bar{b}} \quad (12)$$

$$K_{oq}K_{\bar{q}q} = K_{qo}K_{q\bar{q}} \quad (13)$$

$$K_{bo}K_{b\bar{q}} = K_{oq}K_{\bar{b}q} \quad (14)$$

$$K_{po}K_{p\bar{q}} = K_{oq}K_{\bar{p}q} \quad (15)$$

$$K'_{ob}K'_{\bar{q}b} = K'_{qo}K'_{q\bar{b}} \quad (16)$$

$$K'_{ob}K'_{\bar{b}b} = K'_{bo}K'_{b\bar{b}} \quad (17)$$

$$K'_{ob}K'_{\bar{p}b} = K'_{po}K'_{p\bar{b}} \quad (18)$$

The enzyme velocity may be defined as

$$\begin{aligned} v &= k_1(\mathrm{AEO}) + k_2(\mathrm{AEB}) \\ &= k_1f_1\sum E + k_2f_2\sum E \\ &= (\sum E)(k_1f_1 + k_2f_2) \end{aligned} \quad (19)$$

Since $\sum E = E_t\sum E/(\sum E + \sum F)$, substitution of $\sum E$ by the expression obtained from the King–Altman method as modified by Cha (1968) results in

$$v = \frac{E_t(k_1f_1 + k_2f_2)(k_3f_3 + k_4f_4 + k_5f_5 + k_6f_6)}{k_1f_1 + k_2f_2 + k_3f_3 + k_4f_4 + k_5f_5 + k_6f_6} \quad (20)$$

Substitutions of eq 1–8 into eq 20 followed by appropriate rearrangements give the rate equation in terms of kinetic constants.

$$v = \frac{E_tAB}{K_{ao}K'_{ob}} \Bigg/ \left[(\text{coef 1})\frac{A}{K_{ao}} + (\text{coef 2})\frac{B}{K'_{ob}} + (\text{coef 3})\frac{AB}{K_{ao}K'_{ob}}\right] \quad (21)$$

where

$$\text{coef 1} = \left[\left(1 + \frac{P}{K'_{po}} + \frac{Q}{K'_{qo}} + \frac{B}{K'_{bo}}\right) + \frac{B}{K'_{ob}}\left(1 + \frac{P}{K'_{\bar{p}b}} + \frac{Q}{K'_{\bar{q}b}} + \frac{B}{K'_{\bar{b}b}}\right)\right] \Bigg/ \left(k_3 + \frac{k_4P}{k'_{\bar{p}b}} + \frac{k_5Q}{K'_{\bar{q}b}} + \frac{k_6B}{K'_{\bar{b}b}}\right) \quad (22)$$

$$\text{coef 2} = \left[\left(1 + \frac{P}{K_{po}} + \frac{Q}{K_{qo}} + \frac{B}{K_{bo}}\right) + \frac{B}{K_{ob}}\left(1 + \frac{P}{K_{\bar{p}b}} + \frac{Q}{K_{\bar{q}b}} + \frac{B}{K_{\bar{b}b}}\right) + \frac{Q}{K_{oq}}\left(1 + \frac{P}{K_{\bar{p}q}} + \frac{Q}{K_{\bar{q}q}} + \frac{B}{K_{\bar{b}q}}\right)\right] \Bigg/ \left(k_1 + \frac{k_2B}{K_{a\bar{b}}}\right) \quad (23)$$

$$\text{coef 3} = \left(1 + \frac{B}{K_{a\bar{b}}}\right) \Bigg/ \left(k_1 + \frac{k_2B}{K_{a\bar{b}}}\right) \quad (24)$$

A double-reciprocal form of eq 21 (plot of $1/v$ vs. $1/A$) can be represented by

$$1/v = (\text{slope})(1/A) + (\text{intercept}) \quad (25)$$

where

$$\text{slope} = \left[K_{ao}\Big/\left[E_t\left(k_1 + \frac{k_2B}{K_{a\bar{b}}}\right)\right]\right]\left[\left(1 + \frac{B}{K_{bo}}\right) + \frac{B}{K_{ob}}\left(1 + \frac{B}{K_{\bar{b}b}}\right) + \frac{P}{K_{po}}\left(1 + \frac{B}{K_{p\bar{b}}}\right) + \frac{Q}{K_{oq}}\left(1 + \frac{B}{K_{\bar{b}q}}\right) + \frac{Q}{K_{qo}}\left(1 + \frac{B}{K_{ob}}\right) + \frac{PQ}{K_{\bar{p}q}K_{oq}} + \frac{Q^2}{K_{oq}K_{\bar{q}q}}\right] \quad (26)$$

$$\text{intercept} = \frac{1}{E_t}\left[\left(1 + \frac{B}{K_{a\bar{b}}}\right)\Big/\left(k_1 + \frac{k_2B}{K_{a\bar{b}}}\right) + \left[\left(1 + \frac{B}{K'_{bo}}\right) + \frac{B}{K'_{ob}}\left(1 + \frac{B}{K'_{\bar{b}b}}\right) + \frac{P}{K'_{po}}\left(1 + \frac{B}{K'_{p\bar{b}}}\right) + \frac{Q}{K'_{qo}}\left(1 + \frac{B}{K'_{q\bar{b}}}\right)\right]\Big/\left[\frac{B}{K'_{ob}}\left(k_3 + \frac{k_4P}{K'_{pb}} + \frac{k_5Q}{K'_{qb}} + \frac{k_6B}{K'_{\bar{b}b}}\right)\right]\right] \quad (27)$$

The double-reciprocal plot of $1/v$ vs. $1/B$, on the other hand, cannot be written in a linear form, indicating that the plot in general would not be a straight line. Under certain conditions, however, approximations of the equation become linear. If Ado binds to the MgATP site much less tightly than to the Ado site, it follows that, at a sufficiently low range of Ado concentrations, the terms responsible for such bindings (e.g., $K_{\bar{b}b}$) can be neglected. Even so, in order to have a linear double-reciprocal plot, the concentrations of B must be sufficiently high so that $k_1 \ll k_2B/K_{a\bar{b}}$ or sufficiently low so that $k_1 \gg k_2B/K_{a\bar{b}}$.

Let a linear approximation form of the plot of $1/v$ vs. $1/B$ be

$$1/v = (\text{slope})(1/B) + (\text{intercept}) \quad (28)$$

At a concentration range of B where the binding of Ado to MgATP site is negligible, the terms, $B/K_{bo}$, $B/K_{\bar{b}b}$, $B/K'_{bo}$, $B/K'_{\bar{b}b}$, and $B/K_{\bar{b}q}$ may be eliminated from eq 22 and eq 23.

When $k_1 \ll k_2B/K_{a\bar{b}}$, $k_1$ may also be eliminated from eq 23 and eq 24. Thus, the parameters of eq 28 become

$$\text{slope} = \frac{K_{a\bar{b}}}{k_2E_t}\left[1 + \frac{k_2K'_{ob}}{K_{a\bar{b}}}\left(1 + \frac{P}{K'_{po}} + \frac{Q}{K'_{qo}}\right)\Big/\left(k_3 + \frac{k_4P}{K'_{pb}} + \frac{k_5Q}{K'_{qb}}\right) + \frac{K_{ao}}{A}\left[\left(1 + \frac{P}{K_{po}} + \frac{Q}{K_{qo}}\right) + \frac{Q}{K_{oq}}\left(1 + \frac{P}{K_{\bar{p}q}} + \frac{Q}{K_{\bar{q}q}}\right)\right]\right] \quad (29)$$

$$\text{intercept} = \frac{1}{k_2E_t}\left[1 + k_2\left(1 + \frac{P}{K'_{pb}} + \frac{Q}{K'_{qb}}\right)\Big/\left(k_3 + \frac{k_4P}{K'_{\bar{p}b}} + \frac{k_5Q}{K'_{\bar{q}b}}\right) + \frac{K_{\bar{a}b}}{A}\left(1 + \frac{P}{K_{\bar{p}b}} + \frac{Q}{K_{\bar{q}b}}\right)\right] \quad (30)$$

In this case, both slope and intercept would be a function of $A$ in accordance with the data in Figure 4.

On the other hand, when $k_1 \gg k_2B/K_{a\bar{b}}$, the terms $k_2B/K_{a\bar{b}}$ may be neglected from eq 23 and eq 24. In this case, the equation for the double-reciprocal plot is represented by

$$\frac{1}{v} = \frac{K'_{ob}}{E_t}\left[\left(1 + \frac{P}{K'_{po}} + \frac{Q}{K'_{qo}}\right)\Big/\left(k_3 + \frac{k_4P}{K'_{\bar{p}b}} + \frac{k_5Q}{K_{\bar{q}b}}\right)\right]\left(\frac{1}{B}\right) + \frac{1}{k_1E_t}\left[1 + k_1\left(1 + \frac{P}{K'_{\bar{p}b}} + \frac{Q}{K'_{\bar{q}b}}\right)\Big/\left(k_3 + \frac{k_4P}{K'_{\bar{p}b}} + \frac{k_5Q}{K'_{\bar{q}b}}\right) + \frac{K_{ao}}{A}\left[\left(1 + \frac{P}{K_{po}} + \frac{Q}{K_{qo}}\right) + \frac{Q}{K_{oq}}\left(1 + \frac{P}{K_{\bar{p}q}} + \frac{Q}{K_{\bar{q}q}}\right)\right]\right] \quad (31)$$

The slope of a double-reciprocal plot at such a low range of $B$ would be independent of $A$, which is contrary to the experimental observations shown in Figure 6. Therefore, it may be concluded that the condition $k_1 \ll k_2B/K_{a\bar{b}}$, hence eq 29 and eq 30, holds at the range of Ado concentrations employed in the present studies.

**Registry No.** ATP, 56-65-5; Mg, 7439-95-4; MgATP, 1476-84-2; adenosine, 58-61-7; adenosine kinase, 9027-72-9.

## References


Andres, C. M., & Fox, I. H. (1979) *J. Biol. Chem. 254*, 11388–11393.

Bradford, M. M. (1976) *Anal. Biochem. 72*, 248–254.

Caputto, R. (1951) *J. Biol. Chem. 189*, 801–814.

Cha, S. (1968) *J. Biol. Chem. 243*, 820–825.

Chang, C.-H., Brockman, R. W., & Bennett, L. L., Jr. (1980) *J. Biol. Chem. 255*, 2366–2371.

Cleland, W. W. (1967) *Adv. Enzymol. Relat. Areas Mol. Biol. 29*, 1–32.

Cleland, W. W. (1973) *J. Biol. Chem. 248*, 8353–8355.

DeJong, J. W. (1977) *Arch. Int. Physiol. Biochim. 85*, 557–569.

Divekar, A. Y., & Hakala, M. T. (1971) *Mol. Pharmacol. 7*, 663–673.

Fox, I. H., & Kelley, W. N. (1978) *Annu. Rev. Biochem. 47*, 655–686.

Henderson, J. F., Mikoshiba, A., Chu, S. Y., & Caldwell, I. C. (1972) *J. Biol. Chem. 247*, 1972–1975.

Henderson, J. F., Scott, F. W., & Lowe, J. K. (1980) *Pharmacol. Ther., Part A 8*, 573–604.

Hoffmann, P. J., & Blakley, R. L. (1975) *Biochemistry 14*, 4804–4812.

Leibach, T. K., Spiess, G. I., Neudecker, T. J., Peschke, G. J., Puchwein, G., & Hartmann, G. R. (1971) *Hoppe-Seyler's Z. Physiol. Chem. 352*, 328–344.

Lindberg, B. (1969) *Biochim. Biophys. Acta 185*, 245–247.

Lindberg, B., Klenow, H., & Hansen, K. (1967) *J. Biol. Chem. 242*, 350–356.

Miller, R. L., Adamczyk, D. L., & Miller, W. H. (1979) *J. Biol. Chem. 254*, 2339–2345.

Murray, A. W. (1968) *Biochem. J. 106*, 549–555.

Namm, D. H., & Leader, J. P. (1973) *Anal. Biochem. 58*, 511–524.

Northrop, D. B. (1969) *J. Biol. Chem. 244*, 5808-5819.
Palella, T. D., Andres, C. M., & Fox, I. H. (1980) *J. Biol. Chem. 255*, 5264-5269.
Schaeffer, H. J., & Schwender, C. F. (1974) *J. Med. Chem. 17*, 6-8.
Schmidt, G., Walker, R. D., & Königk, E. (1974) *Tropenmed. Parasitol. 25*, 301-308.
Schnebli, H. P., Hill, D. L., & Bennett, L. L., Jr. (1967) *J. Biol. Chem. 242*, 1997-2004.
Segal, I. H. (1975) *Enzyme Kinetics, Behavior and Analysis of Rapid Equilibrium and Steady-State Enzyme Systems*, p 626, Wiley, New York.
Shimizu, H., Tanaka, L., & Kodama, T. (1972) *J. Neurochem. 19*, 687-698.
Woo, P. W. K., Dion, H. W., Lange, S. M., Dahl, F. L., & Durham, L. J. (1974) *J. Heterocycl. Chem. 11*, 641-643.
Yamada, Y., Goto, H., & Ogasawara, N. (1980) *Biochim. Biophys. Acta 616*, 199-207.
Yamada, Y., Goto, H., & Ogasawara, N. (1981) *Biochim. Biophys. Acta 660*, 36-43.

# Facile Oxygen Exchanges of Phosphoenolpyruvate and Preparation of [$^{18}$O]Phosphoenolpyruvate†

Clifford C. O'Neal, Jr.,*‡ Gary S. Bild, and Linda Tombras Smith

ABSTRACT: Phosphoenolpyruvate when heated in acidic solution exchanges its phosphoryl and carboxyl oxygens rapidly and its enolic oxygen much more slowly with oxygens from water. The incorporation of $^{18}$O into phosphoenolpyruvate was measured by gas chromatography–mass spectrometry and phosphorus-31 nuclear magnetic resonance after heating in $H_2{}^{18}O$ at 98 °C. The rates of exchange of all six oxygens of phosphoenolpyruvate with water increase with increasing acidity, and the phosphoryl oxygens exchange more rapidly than the carboxyl oxygens. The rate of exchange of each oxygen of the phosphoryl group is 16-fold greater than the hydrolysis rate at 1 N HCl. This provides a simple and useful method for the synthesis of [$^{18}$O]phosphoenolpyruvate highly enriched in its phosphoryl-group oxygens. An enrichment of 89% was obtained with a 50% yield. The [$^{18}$O]-phosphoenolpyruvate showed a binomial distribution of $^{18}$O in the phosphoryl-group oxygens. The exchange may be explained by the reversible formation of a transient cyclic phosphate and, for exchange of the enolic oxygen, a transient acyl phosphate. Preparation of [$^{18}$O]phosphoenolpyruvate from [$^{18}$O]$P_i$ by a chemical synthesis from β-chlorolactate was not satisfactory because of drastic loss of $^{18}$O during the procedures used. Some loss of $^{18}$O also occurred during an enzymic synthesis with KCNO, [$^{18}$O]$P_i$, carbamate kinase, and pyruvate kinase.

For studies of oxygen exchanges accompanying cleavage of [$^{18}$O]ATP, it is desirable to have [$^{18}$O]phosphoenolpyruvate to serve for regeneration of the [$^{18}$O]ATP by the pyruvate kinase reaction. Phosphoenolpyruvate synthesized from [$^{18}$O]$P_i$ by a chemical procedure was found to contain much less $^{18}$O than the starting [$^{18}$O]$P_i$. This prompted us to examine the exchange properties of phosphoenolpyruvate in aqueous solution. The results reported herein show that the exchange of the phosphoryl-branch oxygens (those of the $-PO_3$ group) was more rapid than the hydrolysis and, further, that the carboxyl oxygens, and to a lesser extent the enolic bridge oxygen, also underwent exchange with water during heating at acid pH. These exchanges were in part predictable, on the basis of the exchange accompanying hydrolysis reported by Schray & Benkovic (1971) and the facile demethylation of (dimethylphospho)enolpyruvic acid in water. Promotion of demethylation by lower pH was noted by Clark & Kirby (1963) and documented more fully by Stubbe & Kenyon (1972). An even more rapid demethylation of (dimethylphospho)enol-3-bromopyruvic acid occurs (Stubbe & Kenyon, 1971). In addition to revealing interesting properties of phosphoenolpyruvate, the exchange serves as a method for preparation of highly $^{18}$O-labeled phosphoenolpyruvate.

## Experimental Procedures

*Materials.* The monopotassium salt of phosphoenolpyruvate, pyruvate kinase, glycerol kinase, ADP, and Sephadex were purchased from Sigma, and the $^{18}$O-enriched water was from Norsk-Hydro and Monsanto. Dowex and Chelex resins were products of Bio-Rad. All other reagents were of the highest quality commercially available. For preparation of stock HCl in $H_2{}^{18}O$, for use in the synthesis of [$^{18}$O]-phosphoenolpyruvate, 0.4 mL of $H_2{}^{18}O$ of at least 96% enrichment was added to a small vial fitted with a Teflon-lined cap in a dry box. The vial was transferred to a hood and the cap replaced by a cork containing two small holes fitted with glass tubing drawn to a small diameter. One tube was connected by a piece of Teflon tubing to discharge near the rear of the hood; the other was connected, via tubing that had been flushed with nitrogen, to a tank of dry HCl gas. The surface of the enriched water was exposed to the dry HCl gas for 15 min and total acidity (about 12 N) determined by titration of a small aliquot.[1] A similar procedure was employed on

† From the Department of Chemistry and Biochemistry and the Molecular Biology Institute, University of California, Los Angeles, California 90024. *Received May 20, 1982; revised manuscript received October 18, 1982.* This research was supported by Grant GM 11094 to Prof. Paul D. Boyer from the Institute of General Medical Sciences, National Institutes of Health, and by Department of Energy Contract DE-AT03-76ER70102. The NMR spectra were recorded on a Bruker WM-500 instrument at the Southern California Regional NMR Facility at the California Institute of Technology supported by National Science Foundation Grant CHE-7916324 and at the UCLA Department of Chemistry on a 200-MHz instrument provided in part by NSF Grant PCM 75-18884. The high-resolution mass spectra were recorded at the UCLA Department of Chemistry on an instrument purchased in part with funds provided in part by the NSF.

‡ Postdoctoral Fellow of the American Heart Association, Los Angeles affiliate (1980-1981), and of the U.S. Public Health Service (1981-1982).

0006-2960/83/0422-0611$01.50/0 